Purdue University
Purdue e-Pubs

International Refrigeration and Air Conditioning Conference

School of Mechanical Engineering

2006

Thermodynamic Cycle Analysis of Air-to-Water CO2 Heat Pumps

Lili Zhang
United Technologies Research Center

Siva Gopalnarayanan
United Technologies Research Center

Tobias Sienel
United Technologies Research Center

Thermodynamic Cycle Analysis of Air-to-Water CO2 Heat Pumps

Lili Zhang
United Technologies Research Center
411 Silver Lane, East Hartford, CT 06108
Tel: 860-610-1537, Fax: 860 -660-1481, zhangL1@utrc.utc.com

Siva Gopalnarayanan *
United Technologies Research Center
411 Silver Lane, East Hartford, CT 06108
Tel: 860-610-1543, Fax: 860 -660-1140, gopalns@utrc.utc.com

Tobias Sienel
United Technologies Research Center
411 Silver Lane, East Hartford, CT 06108
Tel: 860-610-7181, Fax: 860-660-1378, sienelth@utrc.utc.com

*Corresponding author

ABSTRACT

The objective of this study is to evaluate the performance of Carbon Dioxide (CO_2) air-to-water heat pumps for hydronic space and service water heating applications. Analysis of 15 different cycle configurations is performed based on computer simulations. Results indicate that for both applications, the two stage cycle with a phase separator offered the highest performance. For service heating, the incremental COP over the basic single stage cycle is small (4.459 Vs. 4.371) when heating water from 12°C to 60°C at an outdoor temperature of 10°C. For hydronic space heating applications, the COP of two stage cycles with phase separator is up to 9% higher than the basic cycle (2.724 at an ambient temperature of 0°C while heating water from 30°C to 60°C).

1. INTRODUCTION

In Europe, the most widely employed systems for space heating use a hydronic loop in conjunction with an oil or gas fired boiler. The typical water supply and return temperatures range between 30-50°C and 60-80°C respectively. For service water heating applications, electric heating accounts for nearly 60% while oil or gas provide for the remaining with typical delivery temperatures of about 60-80°C.

In hydronic heating application, a large number of the boilers are between ten and thirty years old and many of them need to be replaced in the near future. This offers an opportunity to introduce a new hydronic heat pump product that uses CO_2 as a refrigerant. CO_2, a naturally occurring fluid, possesses many desirable characteristics including high specific heat, high volumetric heat capacity and, in general, excellent thermodynamic and transport properties. CO_2 was used as a refrigerant until the 1930s, but was then replaced by the Chlorofluorocarbons (CFCs) and Hydrochlorofluorocarbons (HCFCs) that offered lower absolute pressures and higher efficiencies in conventional vapor compression cycles. With the growing awareness of the dual threats of ozone depletion and global warming, significant research activity has been directed to the identification and development of environmentally benign refrigerants. CO_2 has gained lot of attention as a potential refrigerant for automobile air conditioners as well as heat pumps.

A CO_2 heat pump/refrigeration cycle is different from conventional refrigeration cycle in that the heat rejection in a CO_2 system occurs above the critical point while the evaporation occurs below the critical point. The critical temperature and pressure of CO_2 are 31.1°C, 7345 kPa respectively. The basic components of a CO_2 heat pump consist of a compressor, gas cooler, expansion valve, and evaporator. The heat rejection process in the gas cooler occurs without change of phase and consequently there is a change in temperature of the CO_2 gas as it gets cooled.

This temperature profile can be matched with that of the cooling medium (e.g. water) to achieve high delivery temperatures. Operation in the transcritical mode offers the CO_2 system an additional degree of freedom - the pressure and temperature of the heat rejection process can be independently controlled. Thus, unlike conventional refrigerants, such as Hydrofluorocarbons (HFCs), which have a limitation in achieving high water temperatures, in CO_2 systems, the heat rejection pressure can be controlled to achieve the desired heat rejection temperature. Using a CO_2 heat pump, water temperatures as high as 80°C can be achieved without significant loss in Coefficient of Performance (COP).

2. SIMULATION MODEL

About 180 different cycle configurations were identified and 15 cycles shown in Figure 1 were short-listed for further evaluation. The steady state performance of these cycles were evaluated using a reduced order model developed using Engineering Equation Solver [*EES, 2001*].

2.1 Main Program

The cycle configuration is defined and the system operating conditions are specified in the main program which calls the individual component modules. Inputs to the main program include the air temperature and pressure, the water volumetric flow rate and inlet pressure, the water supply and return temperatures, compressor suction superheat, gas cooler discharge pressure as well as the approach temperature difference of the gas cooler. In a two-stage vapor compression cycle, intermediate pressure is specified as well. In a cycle with an intercooler, either the fraction of the total water going to the intercooler (water split ratio for the water-cooled intercooler), or the heat capacity of the intercooler for the air-cooled, need to be specified. In the economizer cycles, the economizer split ratio is a parameter that specifies how the total flow exiting the gas cooler is split between the two sides of the economizer.

2.2 Component Models

2.2.1 Compressor

The inputs to the compressor model are the suction pressure, discharge pressure, suction temperature, compressor displacement and RPM. Outputs of the compressor model are the discharge temperature, mass flow rate of the refrigerant and compressor work. The isentropic and volumetric efficiencies as a function of the pressure ratio are specified in the compressor module. This model is based on the work of *Rieberer* and *Halozan* [1998]:

$$\eta_{is} = 0.00280845 \times pr^5 - 0.0616415 \times pr^4 + 0.52838 \times pr^3 - 2.2132788 \times pr^2 + 4.4938 \times pr - 2.71562 \tag{1}$$

$$\eta_{vol} = -0.00650155 \times pr^2 - 0.0094066 \times pr + 0.93917957 \tag{2}$$

$$\eta_{vol} = \frac{\dot{m}_{actual}}{\dot{m}_{theorectical}} = \frac{\dot{m}_{actual}}{RPM \times V_{displacement} \times \rho_{suction}} \tag{3}$$

$$\eta_{is} = \frac{\dot{W}_{refri\_isentropic}}{\dot{W}_{refri}} = \frac{\dot{m}_{actual} \times (h_{dis} - h_{suction})}{\dot{m}_{actual} \times (h_{dis,is} - h_{suction})} \tag{4}$$

2.2.2 Evaporator

The plate fin round tube evaporator is modeled with a moving boundary heat exchanger using the UA-LMTD [*Incorpera* and *DeWitt, 1990*] method with both evaporator surface area and air flow rate allocated proportionally to the capacities of the two-phase and superheated regions. The airside is assumed to be dry with no frosting. Due to convergence constraints, for this study, zero pressure drop was assumed for both the refrigerant and air flows. Inputs into the evaporator model include mass flow rate of refrigerant, inlet pressure of the refrigerant, quality of the refrigerant at inlet, inlet temperature and pressure of the air and the degree of superheat. The outputs of the model are the total evaporator capacity, outlet temperature and pressure of the refrigerant, air temperature and pressure at the outlet. The air-side heat transfer coefficient is assumed to be constant at 0.7 kW/(m^2•K) [*ASHARE*,1997]. Modified Bennett-Chen correlation [*Hwang et al. 1997*] is used to calculate the heat transfer coefficient for the in-tube evaporation of CO_2:

$$h_{mbc} = (s_{mbc})h_{nb,mbc} + (F)h_{fc,mbc} \tag{5}$$

where, $h_{nb,mbc} = 0.00122\left(\frac{k_l^{0.79} C_{p,l}^{0.5} \rho_l^{0.49}}{\sigma^{0.6} \mu_l^{0.29} h_{fg}^{0.24} \rho_v^{0.24}}\right)\left[T_w - T_{sat}(P_{evap})\right]^{0.4}\left[P_{sat}(T_w) - P_{evap}\right]^{0.75}$ (6)

$$S_{nb,mbc} = \frac{1-\exp(-Fh_l X_o / k_l)}{Fh_l X_o / k_l} \tag{7}$$

$$X_o = 0.05\left(\frac{\sigma}{g(\rho_l - \rho_v)}\right)^{0.5} \tag{8}$$

$$F = \begin{cases} 1.0 & \text{if } X_{tt} \geq 10.0 \\ 2.35(0.213 + x^{-1.0})^{0.736} & X_{tt} \leq 10.0 \end{cases} \tag{9}$$

$$X_{tt} = \left(\frac{\mu_l}{\mu_v}\right)^{0.1}\left(\frac{\rho_v}{\rho_l}\right)^{0.5}\left(\frac{1-x}{x}\right)^{0.9} \tag{10}$$

$$h_l = 0.023\left(\frac{k_l}{D_i}\right)\mathrm{Re}_l^{0.8}\,\mathrm{Pr}_l^{0.4} \tag{11}$$

$$h_{fc,mbc} = h_l\,\mathrm{Pr}_l^{0.6} \tag{12}$$

$$\mathrm{Re}_l = \frac{GD_i}{\mu_l} \tag{13}$$

$$\mathrm{Pr}_l = \frac{C_{p,l}\mu_l}{k_l} \tag{14}$$

The energy balance equations are:

$$Q = UA \times LMTD \tag{15}$$

$$Q = \dot{m}_{ref}(h_{outlet,ref} - h_{inelt,ref}) \tag{16}$$

$$Q = \dot{m}_{air}(h_{inlet,air} - h_{outlet,air}) \tag{17}$$

and, $A = C_1 \times Q$ (18)

where C_1 = 3.5 m^2/kW.

2.2.3 Gas cooler

The gas cooler is modeled as a counter-current, tube-in-tube copper heat exchanger with UA-LMTD method. The inputs to the gas cooler model are the refrigerant mass flow rate, the refrigerant inlet pressure and temperature, water inlet temperature and pressure, mass flow rate of water and approach temperature difference. It is assumed that the pinch point occurs at the outlet of the gas cooler, although the pinch point could occur at the point of inflection in the CO_2 temperature profile. Outputs of the gas cooler model include the gas cooler capacity, water outlet temperature and pressure, refrigerant outlet temperature and pressure. Zero pressure drop is assumed for both the refrigerant and water flows. The calculation of heat transfer coefficient of the supercritical CO_2 region is based on the correlation proposed by *Krasnoshchekov* [1969]:

$$Nu_w = Nu_{ow}\left(\frac{\rho_w}{\rho_b}\right)^n\left(\frac{\bar{c}_p}{c_{p,w}}\right)^m \tag{19}$$

where Nusselt number is evaluated at tube wall temperature,

$$Nu_{ow} = \frac{(f/8)\mathrm{Re}_d\,\mathrm{Pr}}{1.07 + 12.7(f/8)^{0.5}(\mathrm{Pr}^{2/3} - 1)} \tag{20}$$

the friction factor f for smooth tube is:

$$f = (1.82\log_{10}\mathrm{Re}_D - 1.64)^{-2} \tag{21}$$

$$\bar{c}_p = \frac{(h_{bulk} - h_w)}{T_{bulk} - T_w} \tag{22}$$

$$m = B\left(\frac{\overline{C}_p}{C_{pw}}\right)^k \tag{23}$$

where factor B and exponents k and n are empirically determined variables, which are a function of pressure (Table 1).

Table 1: Lookup table for constants to calculate the CO_2 heat transfer coefficient

	Pressure ratio, P/P_critical					
Pr	1	1.1	1.2	1.4	1.6	1.8
B	0.6	0.8	0.9	0.98	1.0	1.0
N	0.2	0.42	0.58	0.7	0.8	0.83
K	0.3	0.12	0.08	0.03	0.01	0

The water side heat transfer coefficient is calculated using McAdams correlation for annular flow [*McAdams,1973*]:

$$\frac{h}{C_p G}\left(\frac{C_p \mu}{k}\right)^{2/3}\left(\frac{\mu_s}{\mu}\right)^{0.14} = \frac{0.023}{(DeG/\mu)^{0.2}} \tag{24}$$

2.2.4 Expansion Device

The inputs to the expansion valve model are the refrigerant inlet enthalpy and the refrigerant inlet and outlet pressure. Isenthalpic expansion with negligible kinetic and potential energy changes is assumed. The output of the expansion valve model is the refrigerant outlet enthalpy.

2.2.5 Intercooler

The water-cooled intercooler model essentially is the same as the gas cooler model except that the CO_2 may not be in the supercritical region. Hence if it is not in the supercritical region, the heat transfer coefficient is calculated using the empirical correlation as in Eq. 11. Then UA-LMTD method is applied to the water-cooled intercooler to calculate the energy balance. In the air-cooled intercooler model, the intercooler capacity is specified to calculate the corresponding outlet temperature of the refrigerant and air, so that

$$Q_{intercooler} = \dot{m}_{ref}(h_{outlet,ref} - h_{inelt,ref}) \tag{25}$$

$$Q_{intercooler} = \dot{m}_{air}(h_{inlet,air} - h_{outlet,air}) \tag{26}$$

Note that the capacity of the air-cooled intercooler is one of the optimization parameters.

2.2.6 Flash-tank and Phase Separator

A closer look at the flash tank cycles (Cycles #4 and #5) reveals that they really consist of two separate sub-cycles on top of each other. A mass balance around the compressors and the flash tank shows that there is no mass transfer between the two sub-cycles. The inlet vapor to the second stage compressor is always saturated. Theoretically, the flash tank could be replaced by an ideal heat exchanger, evaporating the two-phase flow coming from the first expansion device and condensing the vapor coming from the lower compression stage. However, this consideration is only valid for constant ambient conditions. When the system transits from one steady state to another one due to varying ambient conditions, there is mass transfer between the two sub-cycles in order to adjust for the changing conditions.

The phase separator cycles (Cycles #3 and #6) are similar to the flash cycles in a certain perspective. As in the flash tank cycles, the fluid entering the low-pressure expansion valve has vapor quality of zero. However, the cycles cannot be divided into two sub-cycles because the two pressure stages exchanger mass through the phase separator. Besides, the mixing of outlet of vapor line from phase separator and the stream from the low pressure compressor renders the inlet vapor to the second stage compressor superheated.

The inputs to the models include the inlet enthalpy of either one or two streams, the inlet pressure(s), inlet mass flow rate(s). Outputs include the outlet temperature and enthalpy of the vapor and liquid line. Assumptions include zero pressure drop across the phase separator and zero heat loss to the surroundings. The calculations are mainly the mass balance and energy balances:

$$\sum \dot{m}_{inlet} = \sum \dot{m}_{outlet} \tag{27}$$

$$\sum \dot{m}_{inlet} \times h_{inlet} = \sum \dot{m}_{outlet} \times h_{outlet} \tag{28}$$

2.2.7 Economizer

The economizer is modeled as a tube-in-tube single pass copper heat exchanger. The UA-LMTD method is applied to the heat exchanger to calculate the energy balance. To simplify the calculation, constant heat transfer coefficients are assumed on both the cold and the hot sides. Inputs to the economizer model include the pressure, temperature, mass flow rate for both streams. Again it is assumed there is no pressure drop on either side. Outputs of the economizer model are the temperature and enthalpy of both streams.

3. SIMULATION CONDITIONS

The simulation conditions are shown in Table 2. The pinch point for the gas cooler is 2°C. The superheat at evaporator outlet is 5°C. The fan power and water pumping power are 0.4 kW and 0.1 kW, respectively. With these assumptions, the heating COP, the heating capacity $Q_{heating}$ (Q_{gc} plus $Q_{intercooler}$), the displacement(s) of the compressor, and the necessary gas cooler heat exchanger length were calculated. Then each of the cycles were optimized for maximum heating COP.

Table 2: Evaluation conditions for CO_2 heat pump

	Hydronic Heat Pump	Commercial water Heater
Water return Temperature	30°C	12°C
Water supply Temperature	60°C	60°C
Ambient Air Temperature	0°C	10°C
Water flow rate	8.012×10^{-5} m^3/s	8.012×10^{-5} m^3/s
Total Heating Capacity	10 kW	16.1 kW

4. SIMULATION RESULTS

The simulation results for the two different applications are summarized in Tables 3 and 4. The cycles are ranked in the order of their COP. In general, the performance of the different cycle configurations is very sensitive to the compressor performance map. With the performance correlation used in this study, the compressor isentropic efficiency drops as the pressure ratio falls below 2.5. Consequently, many of the two stage cycles when used for service water heating application, suffer from lower isentropic efficiencies. The two stage cycles offer higher performance than the single stage cycle when the temperature lift is higher as in the case of hydronic space heating application.

4.1 Service Water Heating

The best COP for this application is that of the phase separator cycle (#3), at 4.459. This should be attributed to the fact that the compressor isentropic efficiencies were higher than in the other cycles.

Although the COP for the water intercooled phase separator cycle (#7), is slightly higher than the simple phase separator cycle (#6), the length of the heat exchanger required for this cycle is almost 4 times more to achieve the same gas cooler outlet approach temperature.

The air intercooled cycles, (#15 and #14), do not show any improvement in COP, compared to Cycle #6. This is due to the fact that the improvement on the second stage compressor efficiency due to the intercooling is negated by the increase of the refrigerant mass flow rate and therefore, the compression work, to match the heating capacity when the intercooling decreases the discharge temperature. Air intercooled cycles in general have lower COP since heat that could have been used for heating water is thrown out.

Even though using the air intercooler heat to preheat the air entering the evaporator (Cycle #10) rather than throwing the heat out increases the COP (due to higher evaporation pressures), there is no overall benefit in using any air intercooling for heating applications.

The two-stage water intercooled cycle does not show any improvement compared to the basic cycle. The COP decreases from 4.371 to 3.572. The reason for this is that the compressor efficiencies in the two-staged cycle are lower than that of the basic cycle so that the compressor work is higher.

Even though the superheat for phase separator cycles are higher than the flashed cycles (saturated), the phase separator cycles in general show advantages over the flashed cycles, due to the fact that mass flow rate through the first stage compressor is lower for the phase separator cycles.

The economizer cycles do not show any improvement in COP due to their larger compression work associated with the high discharge pressure.

Based on this analysis, the basic single stage cycle appears to be the best choice for service water heating application. Although the phase separator cycle (#3) offers a 2% higher COP than the basic cycle (#1), the need for additional components (expansion valve and phase separator) may not justify the application of this cycle. One situation where the Cycle #3 may be advantageous is if an interstage expansion tank is used as a charge storage device.

4.2. Hydronic Space Heating

Since the space heating application is evaluated at lower outdoor temperatures (consequently lower evaporating pressures) and also due to the fact that the return water temperature is higher, the expansion losses are higher. Thus, the COPs of CO_2 heat pump for the space heating application are much lower than that of the water heating application. At the evaluation conditions, the highest COP is 2.724, 40% lower than the highest COP of 4.459 in water heating.

In the economizer cycles, the water intercooling did show some improvement in COP because the second stage compressor efficiency is increased and this lead to the reduction of the compression work.

Here again, the air intercooled cycles, (#15 and #14), do not show any improvement in COP, compared to Cycle #6 due to the fact that useful heat is thrown away.

The two-stage water intercooled cycle does not show any improvement compared with the basic cycle. On the contrary, the COP decreases from 2.494 to 2.459. The reason for this is that the compressor efficiencies in the two-staged cycle are lower than that of the basic cycle so that the compressor work is higher.

For space heating applications, the two stage cycles offer potential increases in COP of up to 10% over basic cycle due to the fact that the temperature lift is higher. However, detailed thermoeconomic analysis will have to be performed in order to determine if the higher order cycles provide any significant lower life cycle costs.

The ranking of the cycles is different for the two different applications due to the fact that the application conditions are quite different. This highlights the fact that while designing the system, careful attention should be paid in determining the conditions at which the system is likely to operate most of the time.

6. CONCLUSIONS

In this study, thermodynamic analysis of 15 different CO_2 heat pump cycles is performed. The computer simulation is carried out using the model developed in the Engineering Equation Solver modeling platform. For service water heating application, the basic single stage cycle offers the best solution with a heating COP of 4.459 when heating water from 12°C to 60°C at an outdoor temperature of 10°C. For hydronic space heating applications, the two stage cycles with phase separator offer the highest possible COP at the conditions of evaluation. In this case the heating COP is up to 9% higher than the basic cycle (equal to 2.724 at an ambient temperature of 0°C while heating water from 30°C to 60°C).

NOMENCLATURE

A	area, m^2
C1	constant (in Eq. 18)
COP	Coefficient of Performance
$C_{p,l}$	specific heat of liquid, kJ/(kgK)
$C_{p,w}$	specific heat of liquid at wall temperature, kJ/(kgK)
D	diameter, m
F	forced convection enhancement factor
f	single phase flow friction factor
G	mass flux, kg/(m^2s)
$h_{discharge}$	specific enthalpy of refrigerant at discharge pressure, kJ/kg
$h_{discharge,is}$	isentropic enthalpy of refrigerant at discharge pressure, kJ/kg
$h_{nb,mbc}$	nucleate boiling heat transfer coefficient using modified Bennet-Chen correlation, W/(m2K)
$h_{fc,mbc}$	forced convection heat transfer coefficient calculated using modified Bennet-Chen correlation, W/(m2K)
h_{fg}	latent heat of vaporization, kJ/kg
$h_{suction}$	specific enthalpy of refrigerant at suction pressure, kJ/kg
k_l	thermal conductivity, kJ/(kgK)
LMTD	log mean temperature difference, K
$\dot{m}_{actual}$	mass flow rate of refrigerant, kg/s
$\dot{m}_{theoretical}$	theoretical mass flow rate of refrigerant, kg/s
Pr	Prandtl number
pr	pressure ratio
$P_{sat}(T)$	saturation pressure at temperature T, kPa
Q	heat transfer rate, kW
Re	Reynolds number
RPM	Revolutions Per Minute
S_{mbc}	dimensionless scaling factor
T_w	wall temperature, K
$T_{sat}(P)$	saturation temperature at pressure P, K
U	overall heat transfer coefficient, W/(m^2K)
$V_{displacement}$	displacement volume of compressor, m^3
$\dot{W}$	power, kW
x	two-phase flow vapor quality
X_o	modified Bennett-Chen coefficient
X_{tt}	Lockhart-Martinelli parameter
η_{is}	isentropic efficiency of compressor
η_{vol}	volumetric efficiency of compressor
μ_l	dynamic viscosity of liquid, kg/(ms)
$\rho_{suction}$	refrigerant density at suction, kg/m3
σ	surface tension, N/m

<u>Subscripts</u>

b	bulk
critical	value at critical point
d	diameter
fc	forced convection
is	isentropic
l	liquid
mbc	modified Bennett-Chen
nb	nucleate boiling
ow	tube outside wall
ref	refrigerant
tp	two-phase
v	vapor
vol	volumetric
w	wall

REFERENCES

ASHRAE, 1997, ASHRAE Handbook- Fundamentals. American Society of Heating, Refrigerating and Air-Conditioning Engineers, Inc.

EES, Engineering Equation Solver Ver 6.179, 2001, F-Chart Software, Middleton, WI.

Hwang Y.H. , B. Kim, and R. Radmermacher. 1997, “Boiling Heat Transfer Correlation for Carbon Dioxide,” Heat Transfer Issues in ‘Natural’ Refrigerants (conference), Center for Environmental Energy Engineering, University of Maryland, College Park, MD, USA.

Incorpera. F. D. and D. P. DeWitt, 1990, Fundamentals of Heat Transfer and Mass Transfer, 3rd Ed. New York, John Wiley and Sons.

Krasnoshchekov, E., I. Kuraeva, and V. Protopopov, 1969. “Local heat Transfer of Carbon Dioxide at Supercritical Pressure Under Cooling Conditions,” Teplofizika Vysokikh Temperature 7{5}:922-930.

McAdams, J. A. and D. F. Rogers, 1973, Computer Aided Heat Transfer Analysis. McGraw-Hill, New York.

Rieberer R. and H. Halozan, 1998, “CO2 Heat Pumps in Controlled Ventilation Systems,” Natural working Fluids ’98. International Institute of Refrigeration, Oslo, Norway, pp.2/2-221.

Table 3. Cycle analysis results for hydronic heat pump

Cycle No.	Cycle Description	COP	1st Stage Displacement (cm^3)	2nd Stage Displacement (cm^3)	Isentropic Efficiency (%)	Gas Cooler Pressure (kPa)	Intermediate Pressure (kPa)	*inter /fraction (%)	Gas Cooler length (m)	intercooler length (m)
6	phase separator	2.724	25.74	23.28	73.0/74.2	8053	4094		18.5	
15	phase separator (air int+evap heat)	2.716	26.24	22.88	74.0/72.5	8000	4200		19.69	
14	phase separator (air intercooled)	2.711	26.41	22.88	74.3/72.5	8000	4200		19.63	
3	separator	2.706	35.72	3.026	77.1/38.1	7800	6000		19.69	
4	flash tank	2.688	27.35	20.21	78.1/70.3	8450	4600		135.8	
7	phase separator(water intercooled)	2.671	28.15	19.62	79.4/64.7	8200	4834	40	46.4	0.03
1	basic	2.494	42.13		76.6	8032			14.51	
13	economizer(2) water intercooled	2.464	28.09	17.41	81.0/69.6	10000	5500	50/38.5	26.06	1.10
2	2 stage water intercooled	2.459	35.47	12.07	80.8/58.9	9500	6000	55	151.7	2.42
5	flash tank (water intercooled)	2.416	28.82	17.69	80.9/72.0	10200	5400	21	107	0.15
9	economizer(1) water intercooled	2.414	32.52	8.83	78.8/66.1	12100	7000	36/37	115.8	3.15
10	2stage air intercooled+evap heated	2.408	35.23	19.3	78.7/72.7	9000	4700		12.48	
11	2stage air intercooled	2.402	36.43	20.17	70.7/78.3	8500	4600		13.27	
12	economizer (2)	2.267	31.15	12.11	79.2/68.2	12100	6800	48	13.87	
8	economizer(1)	2.255	32.7	12.67	79.0/55.2	10500	6900	31	18.28	

Table 4. Cycle analysis results for water heating

Cycle No.	Cycle Description	COP	1st Stage Displacement (cm^3)	2nd Stage Displacement (cm^3)	Isentropic Efficiency (%)	Gas Cooler Pressure (kPa)	Intermediate Pressure (kPa)	*inter /fraction (%)	Gas Cooler length (m)	intercooler length (m)
3	separator	4.459	36.76	2.334	81.0/72.8	7500	3915		37.27	
1	basic	4.371	40.07		81	7500			40.19	
7	phase separator(water intercooled)	3.6	36.38	18.97	73.7/53.3	8210	5500	30	154.6	2.04
6	phase separator	3.591	33.29	29.18	50.0/70.4	7500	4080		29.79	
15	phase separator (air int+evap heat)	3.589	32.49	30.72	43.0/73.7	7500	3850		31.01	
14	phase separator (air intercooled)	3.585	32.61	30.73	43.0/73.7	7500	3850		30.95	
2	2 stage water intercooled	3.572	36.23	15.26	78.4/50.5	9000	6200	30	120.8	3.28
4	flash tank	3.547	35.37	23.86	61.3/69.9	8400	4600		403.8	
10	2stage air intercooled + evap heated	3.465	35.73	23.95	67.6/59.8	8000	5000		26.26	
11	2stage air intercooled	3.461	35.86	23.95	67.8/59.8	8000	5000		26.2	
5	flash tank (water intercooled)	3.246	35.98	21.76	67.9/77.0	10500	5000	20	125.1	0.67
9	economizer(1) water intercooled	3.049	36.63	17.88	77.5/76.1	12300	6000	15/29	23.46	0.95
12	economizer(2)	2.992	36.32	18.76	77.5/76.1	12300	6000	33	17.53	
8	economizer(1)	2.991	36.32	18.84	77.5/75.9	12270	6000	32	17.11	
13**	economizer(2) water intercooled	2.868	35.47	23.58	76.2/73.2	11200	5800	44/35	33.19	3.61

* inter: the percentage of total water flow split to water intercooler; fraction: the fraction of total CO_2 flow exiting the gas cooler split to the cool side of the economizer

** with higher minimum temperature difference in the gas cooler than the specified 2K due to problems with convergence.

Figure 1: Cycle configurations evaluated in this study

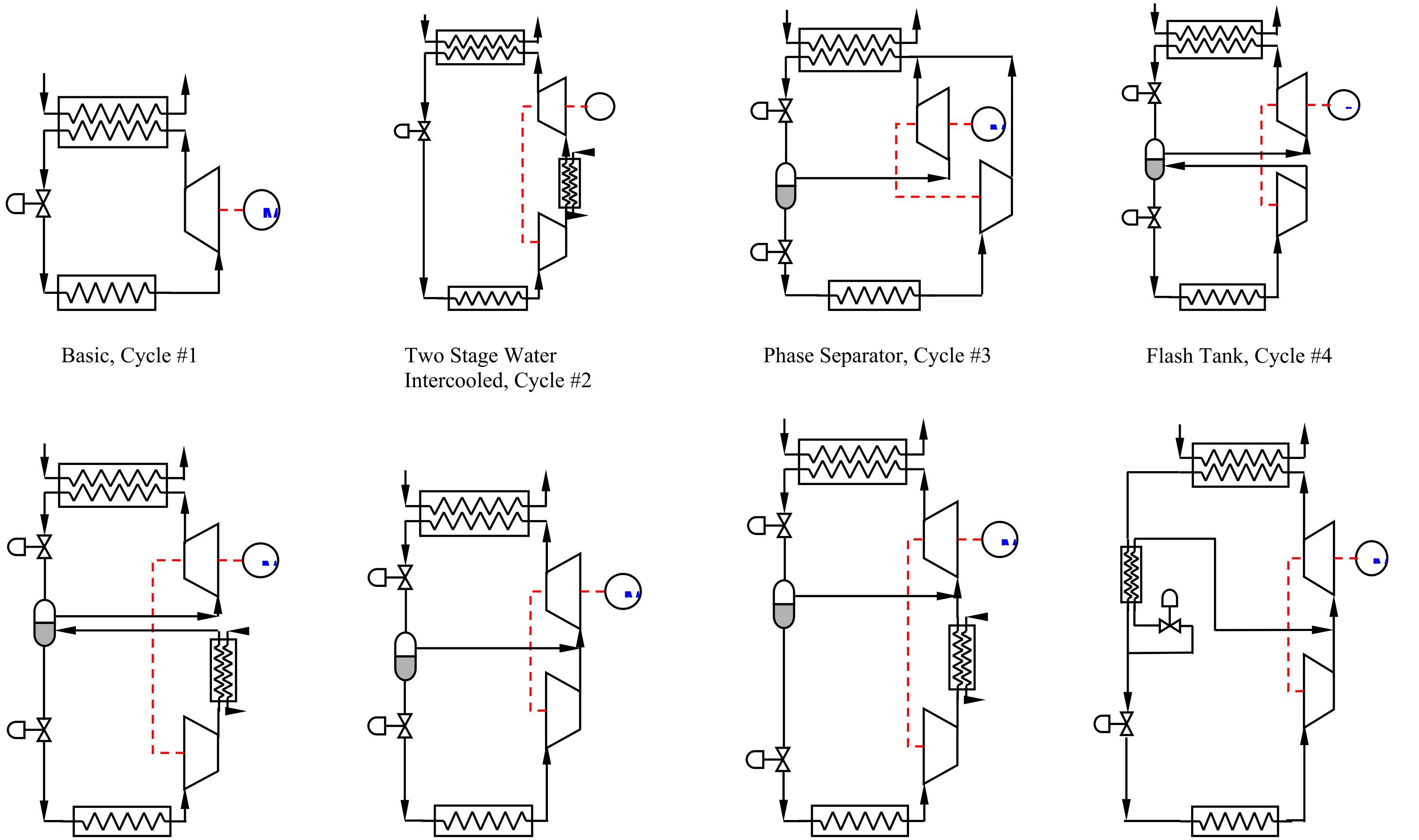

Basic, Cycle #1

Two Stage Water Intercooled, Cycle #2

Phase Separator, Cycle #3

Flash Tank, Cycle #4

Flash Tank w/ Water Intercooler, Cycle #5

Phase Separator, Cycle #6

Phase Separator w/ Water Intercooler, Cycle #7

Economizer 1, Cycle #8

Figure 1 (cont'd): Cycle configurations evaluated in this study

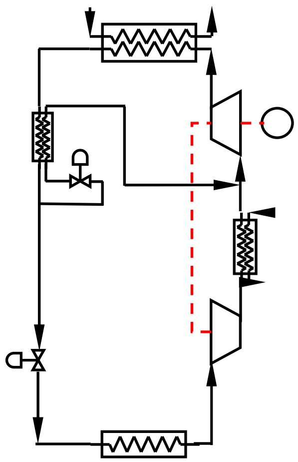

Economizer 1 w/ Water Intercooler, Cycle #9

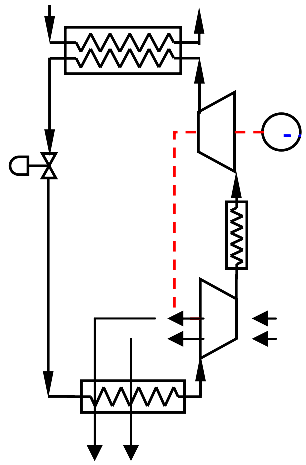

Air Intercooler w/ Evaporator Heating, Cycle #10

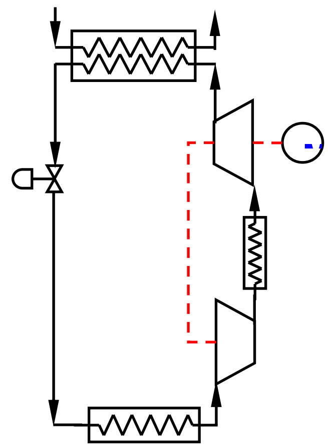

Air Intercooler, Cycle #11

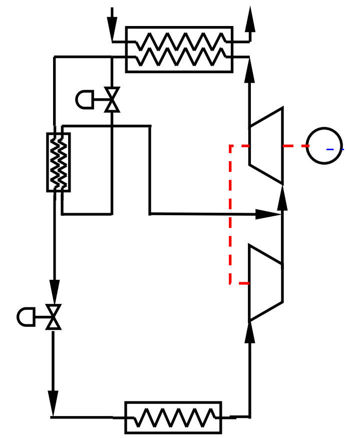

Economizer 2, Cycle #12

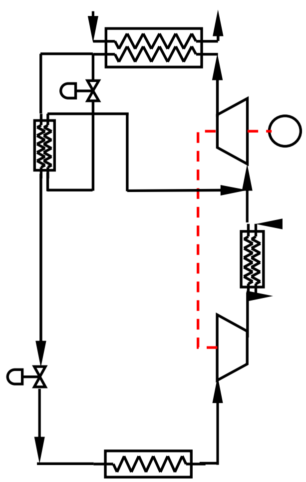

Economizer 2 w/ Water Intercooler, Cycle #13

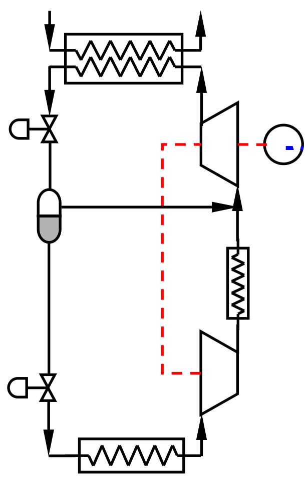

Phase Separator w/ Air Intercooler, Cycle #14

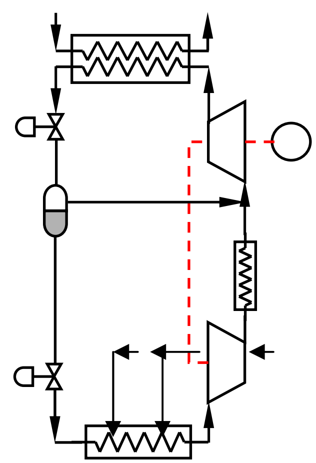

Phase Separator w/ Air Intercooler & Evaporator Heating, Cycle #15